

UDK 539.374+669.715

PACS numbers: 62.20.Fe, 62.20.Hg

## Mechanism of superplastic deformation of high-strength aluminum alloy 1933 with bimodal structure

A.V. Poyda<sup>2</sup>, A.V. Zavdoveev<sup>3,4</sup>, V.P. Poyda<sup>1</sup>, V.V. Bryukhovetskiy<sup>2</sup>,  
D.E. Milaya<sup>1,2</sup>, R.V. Sukhov<sup>1</sup>

<sup>1)</sup> V.N. Karazin Kharkov National University  
Svoboda square, 4, Kharkov, Ukraine, 61077,

<sup>2)</sup> Institute of Electrophysics & Radiation Technologies NAS of Ukraine  
Chernyshevskaya St. 28, P.O. Box 8812, Kharkov, Ukraine, 61002

<sup>3)</sup> Paton Electric Welding Institute of NAS of Ukraine  
Bozhenko St., 11, Kiev, Ukraine, 03680

<sup>4)</sup> Donetsk Institute for Physics and Engineering named after A.A. Galkin NAS of Ukraine  
Nauky Prosp., 46, Kiev, Ukraine, 03028

The characteristics of the initial structural state and phase composition of industrial alloy 1933 are determined. The specific proportion of low-angle boundaries and high-angle boundaries is determined. The mechanism of superplastic deformation of aluminum alloy 1933 with a bimodal structure is considered. In the investigation of the deformation relief the fibrous structures are found, indirectly confirming the presence of a liquid phase during the mechanical tests. The effect of the inclusions of liquid phase, localized at the grain boundaries, on the implementation of deformation and accommodative mechanisms developing during their superplastic flow is analyzed.

**Keywords:** superplasticity, bimodal structure, grain boundaries, fibrous structures, partial melting.

Встановлено характеристики вихідного структурного стану і фазового складу промислового напівфабрикату сплаву 1933. Визначено питому частку малокутових і великокутових меж зерен. Розглянуто механізм надпластичної деформації алюмінієвого сплаву 1933 з бімодальною структурою. При дослідженні деформаційного рельєфу виявлені волокнисті структури, що опосередковано підтверджує наявність рідкої фази під час механічних випробувань. Проаналізовано вплив включень рідкої фази, локалізованих на межах зерен, на здійснення деформаційних і акомодаций механізмів, що розвиваються в ході їх надпластичної деформації.

**Ключові слова:** надпластичність, бімодальна структура, межі зерен, волокнисті структури, часткове плавлення.

Установлены характеристики исходного структурного состояния и фазового состава промышленного полуфабриката сплава 1933. Определена удельная доля малоугловых и большеугловых границ зерен. Рассмотрен механизм сверхпластической деформации алюминиевого сплава 1933 с бимодальной структурой. При исследовании деформационного рельефа обнаружены волокнистые структуры, что косвенно подтверждает наличие жидкой фазы во время механических испытаний. Проанализировано влияние включений жидкой фазы, локализованных на границах зерен, на осуществление деформационных и аккомодационных механизмов, развивающихся в ходе их сверхпластической деформации.

**Ключевые слова:** сверхпластичность, бимодальная структура, границы зерен, волокнистые структуры, частичное плавление.

### Introduction

To show the effect of micro-grain structural superplasticity (SSP) of industrial aluminum alloys must have steady to coarsening ultrafine equiaxed grain structure [1-3]. It is considered that the smaller the initial grain size in the specimen, the greater the area of high angle intergranular (intergrain and interphase) boundaries per volume unit of its working part. Therefore, the greater the

number of grains may be involved in the implementation of grain boundary sliding (GBS) - the main deformation mechanism of superplastic deformation (SPD) [1-3]. Such a structural state in multicomponent aluminum alloys with matrix structure can be obtained by carrying out of their thermomechanical processing. However, using of standard methods of heat treatment to the semifinished products of many commercial aluminum alloys is not always provides

them uniform ultrafine equiaxed structures, so in the initial state they often have bimodal or varying grain size structure [1-4].

High-strength forging alloy 1933 of Al-Zn-Mg-Cu-Zr [5] is widely used in the aircraft industry. Large forgings, stampings and pressed strips for massive elements of the internal skeleton of the power of modern aircraft airframes are produced from it.

A significant disadvantage of this alloy as well as of other high-strength alloys of Al-Zn-Mg-Cu, is that the presence in its composition of high amounts of zinc, magnesium and copper to increase its strength, reduces its plasticity [6]. Low technological plasticity of the alloy 1933 greatly limits its use for the production of complex and thin-walled products needed for the aircraft industry. This disadvantage can be eliminated by the use of superplastic forming, which is a promising technology of materials processing by pressure based on the effect of SSP.

In [7-10] was shown that the alloy 1933 with an initial bimodal structure showed the effect of high-temperature structural superplasticity (HTSS). It is determined that during the SPD GBS developed intensively and occurred not only on ultrafine grain boundaries, but also on the boundaries of large polygonized grains parallel to the direction of strain. It is uncharacteristic for the existing classical conceptions about the development of GBS in terms of micro-grain SSP and can be connected with the presence on grain boundaries of small amounts of liquid phase.

In this paper in order to clarify the mechanism of SPD of alloy 1933, the characteristics of the initial structural state and phase composition of the alloy were studied and the attestation of its grain boundaries was performed.

Based on generalization of the results, obtained in the work, and accounting data available in the literature, the analysis of deformation and accommodative mechanisms of SPD of the alloy is performed.

#### **Materials and methods of the experiment**

Investigated in the paper alloy 1933 has such a chemical composition (1,6 – 2,2% Mg; 0,8 – 1,2% Cu; 0,1% Mn; 0,66 – 0,15% Fe; 0,1% Si; 6,35 – 7,2% Zn; 0,03 – 0,06% Ti; 0,05% Cr; 0,10 – 0,18% Zr; 0,0001 – 0,02% Be; base Al, % wt.) [5]. The main alloying elements in the alloy are magnesium, zinc and copper. They play a fundamental role in the partial melting of superplastic aluminum alloys and as a result, creating small amounts of viscous liquid phase at the grain boundaries during deformation [11-12].

Mechanical tests of the alloy specimens, prepared from industrial intermediates, held in air by stretching them in creep mode at constant flow stress according to the procedure described in detail in [13].

Grain structure, cavity morphology and morphology of fibrous in specimens were studied using light microscopy

(MIM-6 with the digital camera Pro-MicroScan) and scanning electron microscopy (JEOL JSM-840), and standard techniques of quantitative metallography [14].

To determine the proportions of ultrafine and coarse grains, the grain boundary misorientation angles and to make quantitative assessment of their content in the alloy 1933 the electron backscatter diffraction analysis (EBSD) was used [15]. Investigations were performed using a scanning electron microscope JEOL JSM-6490LV, equipped with energy dispersive spectrometry INCA Penta FETx3 and by detector of backscattered electrons Nordlys S.

Analysis of the obtained structures was performed according to the procedure described in [15], using software HKL Channel 5, which is included in the set of technical documents to the microscope.

The surface of the working part of the specimens was subjected to grinding and to mechanical polishing. Surface finishing of sections for metallographic investigations was carried out using a diamond paste grit 1/0.

Specimens which were used for EBSD analysis were subjected to electropolishing. It was performed in a solution of such composition: 40 wt. %  $H_2SO_4$ , 45 wt. %  $H_3PO_4$ , 3 wt. %  $CrO_3$ , 11 wt. %  $H_2O$  [15]. Mode of operation: operating temperature 60-80°C, the anode current density, the voltage of 15-18 V, exposure – a few minutes.

To reveal the grain boundaries during the metallographic studies was used universal chemical etchant of such a composition: 17 ml  $HNO_3$ , 5 ml HF, 78 ml  $H_2O$ . In addition to the chemical etching for revealing of grain boundaries of the working part surface of the test specimens of alloy as the initial one, and superplastically deformed to a certain degree of deformation, strain relief method was used. To determine the contribution of grain boundary sliding (GBS) in the overall deformation and for studying of the kinetics of its development at different stages of SPD used a method of marker scratches. On the polished specimens using a diamond paste of dispersion 3 microns, the marker risks parallel to the axis of their subsequent direction of stretching were applied. Mechanical testing was carried out using specimens in a HTSP in the creep mode, which led to the formation on the surface of polished specimens of a deformation relief as a result of a small (3-5%) deformation. The views of it were studied.

The average grain size  $\langle d \rangle$  was determined by light microscopy photomicrographs with use of random secant method [8]. Full statistical grain size distribution based on the data of EBSD analysis.

#### **Results and Discussion**

Figure 1, a shows a micrograph of a typical view of the initial microstructure of the specimen of 1933 alloy obtained using light microscopy techniques. It is seen that the microstructure of the alloy is bimodal. It consists of

the regions containing a large number of fine recrystallized grains and ultrafine grains with  $\langle d \rangle = 7 \pm 1$  microns, separated by high-angle boundaries (HAB, misorientation angle  $> 10^\circ$ ) of grains and contain some amount of coarse elongated polygonized grains with  $\langle d \rangle = 50 \pm 1$   $\mu\text{m}$ , which are separated by low-angle boundaries (LAB, misorientation angle  $< 10^\circ$ ) of grains.

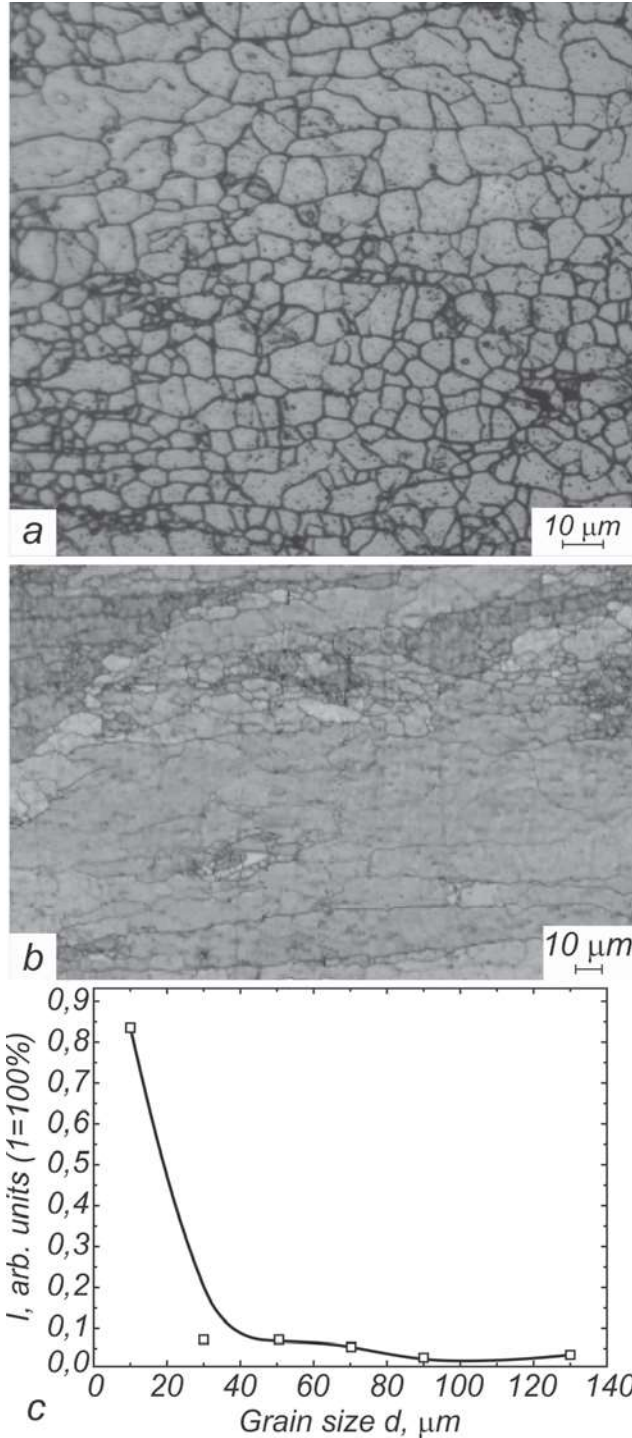


Fig.1. Typical views of the initial microstructure specimen alloy 1933: a – obtained by using light microscopy techniques; b – selected for EBSD analysis; c – the grains size distribution  $\langle d \rangle$  for shown on Fig.1, b fragment of specimen of alloy 1933.

Data of metallographic investigations, obtained using light microscopy method, are qualitatively consistent with the data obtained as a result of EBSD analysis.

Figure 1, b shows the map of contrasts, which was used for quantitative metallographic analysis of the initial structural state of the alloy in the investigated part of the surface of the specimen of alloy 1933. It is seen that the original structure of the alloy is not uniform. It contains large elongated grains, which border on plots occupied by

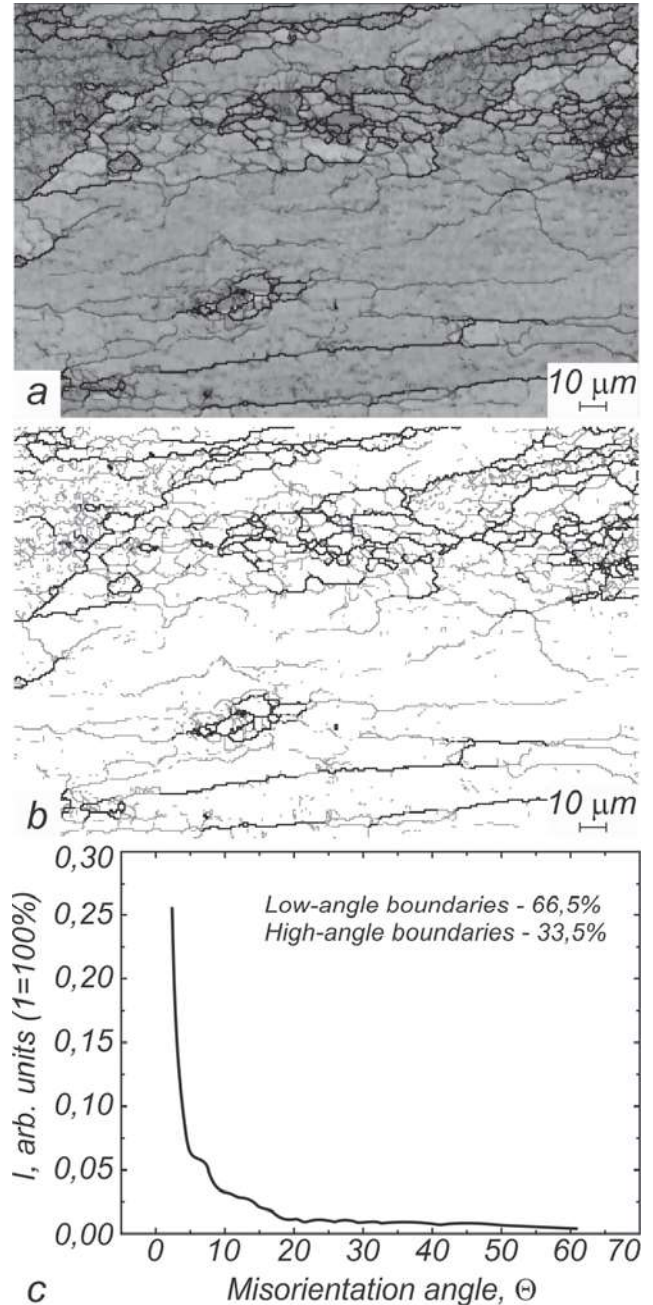


Fig.2. EBSD analysis maps: a – resulted from combination of contrasts map and misorientation angle of grain boundaries map; b – orientation angles of grain boundaries map; c – dependence of the relative amounts of different grain boundary misorientation angle from disorientation for the tested plot of the surface of alloy 1933 specimen.



small and ultra-fine grains.

Figure 1, c shows the distribution of the grain sizes by the magnitude for the investigated part of the alloy 1933 specimen. It is evident that in a bimodal structure identified on the surface of the investigated area, fine and ultra-fine grains dominate and the amount of large polygonized grains is much less.

Figure 2, a shows a fragment of the microstructure, obtained as a result of overlapping of contrasts maps and maps of misorientation angle of grain boundaries, and figure 2, b is a map of orientation angle of grain boundaries. These maps were used to determine the specific proportion of LAB grains and HAB grains for the tested plot of the specimen surface of the alloy 1933.

In Figure 2, c the quantitative distribution of the grain boundaries by misorientation angle is represented. It was built as a result of accounting of all attested grain boundaries existing in the studied area of specimen of alloy 1933. When building this relationship was usually to attribute to the LAB grains those grain boundaries, which have misorientation angle below  $10^\circ$ , and to attribute to the HAB - those grain boundaries, which are misoriented above  $10^\circ$  [15]. It was found that the specific proportion of LAB grains for the tested area is 65.5% and the specific proportion of HABs grains is 35.5%. These data strongly suggest that the original structure of the specimens of alloy

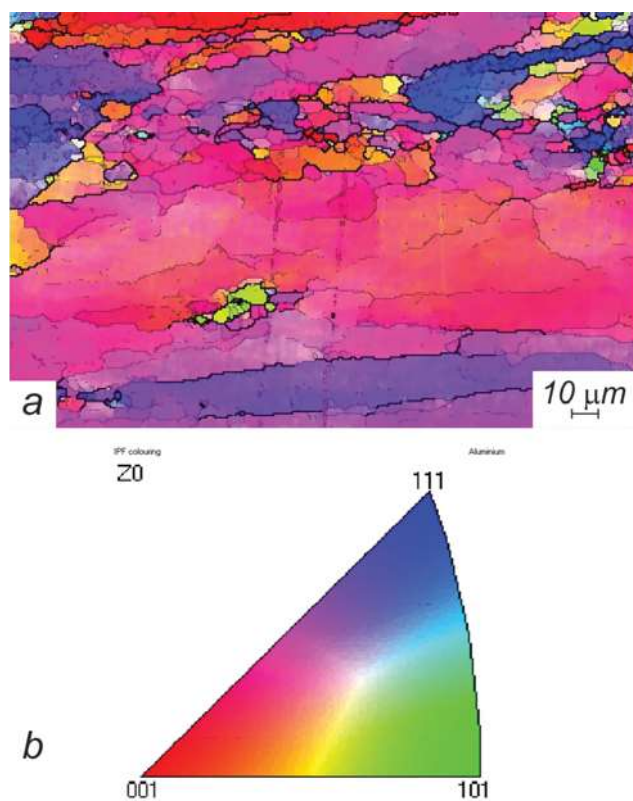


Fig.3. a – orientations of grains map in the investigated area of alloy 1933 specimen; b – image legend for this orientations map.

1933 is not fully recrystallized, and that in it there is a developed substructure.

Figure 3, a shows a map of grains orientations in the investigated area of specimen of alloy 1933, and in Figure 3, b - the image of the legend to it, which was built in the space of inverse pole figures. It is seen that the orientation of the grains in this area are distributed inhomogeneously. For ultrafine grains are prevalent orientations tending to an orientation (111) and (001), and for large polygonized grains, prevailing is orientation, tending to the orientation (001). On the orientations map is also present a number of grains painted in green. Their orientation tends to orientation (101).

Let us analyze the phase composition of alloy 1933 specimens. According to the phase diagram of Al-Mg-Cu-Zn, [6], zinc, magnesium and copper under conditions close to equilibrium form with aluminum and between each other solid solutions and various intermetallic compounds:  $MgZn_2$  ( $\eta$ -phase),  $Al_2CuMg$  (S-phase),  $Mg_3Zn_3Al_2$  (T-phase), which play a significant role in the hardening of the alloy 1933 when heat treated. In addition to these phases in composition of the alloy 1933 in conditions close to equilibrium, must be present fine particles of phase  $ZrAl_3$ , which play an important role in the occurrence of dynamic recrystallization and serve to inhibit grain growth during SPD of aluminum alloys [1-3]. As a result of diffractometric research of initial specimen of the alloy 1933 [7-9], it was found that the intensive diffraction peaks on the diffractogram correspond to the aluminum based solid solution ( $\alpha_{Al}$ -phase). It also revealed a low-intensity diffraction peaks corresponding  $\eta$ -phase ( $MgZn_2$ ) и T-phase ( $Mg_3Zn_3Al_2$ ). This indicates that the amount of  $\eta$ -phase and T-phase in the initial specimen of the alloy is not significant. S-phase and phase  $ZrAl_3$ , which, undoubtedly, are present in the initial specimens of the alloy 1933, were not found by the methods of diffraction. Since the crystallization of alloy ingots of 1933, like other alloys of the Al-Mg-Cu-Zn, takes place in conditions far from equilibrium, so in the structure of the alloy may be present intermetallic particles, which come in various nonequilibrium structural components characteristic of the alloys of this system [6].

As a result of energy dispersive X-ray microanalysis of the initial microstructure of the alloy 1933 the concentration of aluminum, zinc and magnesium at the grain boundaries and in the middle of grain was determined [10]. It is determined that the concentration of zinc and magnesium which is responsible for reducing the temperature of the partial melting of superplastic aluminum alloys [11,12] on individual grain boundaries is higher compared with their average concentration in the material and in the middle of the grains.

The previously mentioned indicates that in the specimens of 1933 alloy prepared for mechanical testing, most of the alloying elements (Mg, Zn) is in the solid

solution based on aluminum. Only in some parts of the grain boundaries, there is an increased concentration of alloying elements.

It was determined [7-10] that during heating of alloy 1933 specimens to a test temperature, partial melting of the alloy takes place. It results in the appearance of metastable viscous liquid phase at grain boundaries.

As a result of mechanical tests carried out in creep mode at a constant flow stress, it was found that the optimal conditions for occurrence of the effect of HTSP for alloy 1933 are as follows: temperature  $T = 520^{\circ}\text{C}$ , flow stress  $\sigma = 5,5 \text{ MPa}$ . Maximum relative elongation of specimen to failure  $\delta$ , superplastically deformed under  $T = 520^{\circ}\text{C}$ ,  $\sigma = 5,5 \text{ MPa}$  and true strain rate  $1,2 \cdot 10^{-4} \text{ s}^{-1}$  was observed as 260% [7-10].

As a result of detailed studies of typical views of deformation relief which formed on the surface of the working part of superplastically deformed alloy 1933 specimens, performed using optical and scanning electron microscopy fibrous structures (see. Fig.4), localized in the cavities and microcracks were found. The formation and development of such structures shows convincingly that the alloy 1933 during SPD was in a solid-liquid state due to partial melting.

The ends of the fibers (see. Fig.4) are connected to the inner surfaces of grains in cavities formed during the separation during of grains, when grains separated one from each other by boundaries during GBS, approximately perpendicular to the strain direction. The number of fibers in cavities is different. It appears to depend on the amount of liquid phase inclusions localized at the grain boundaries, which surround the grain boundary cavities.

As a result of energy dispersive X-ray microanalysis of the chemical composition of the material that makes the fibrous structure formed during SPD of 1933 alloy specimens, was determined [10], that the concentration of Mg in them is increased in comparison with the average concentration in the alloy. This result agrees with the data on the chemical composition of the fibers obtained by the authors of works [16,17] in the study of the structural state of the specimens of aluminum alloys Al-Mg-Cu-Zn, showed HTSP in a solid-liquid state.

On the surface of the fibers and grains to which they are connected, friable oxide films were found. This suggests that during SPD of 1933 alloy specimens tested at a temperature  $T=520^{\circ}\text{C}$  in its working part the dynamic oxidation of the inclusions of liquid material that was present in small amounts at the grain boundaries and at the sliding grain boundary edges intensively occurred.

These thermal studies, which were aimed at investigation of the probable causes of the kinetics of partial melting of the alloy 1933 [9] in the presence of superplastically deformed at  $T = 520^{\circ}\text{C}$  specimens of fibrous structures which comprised an increased

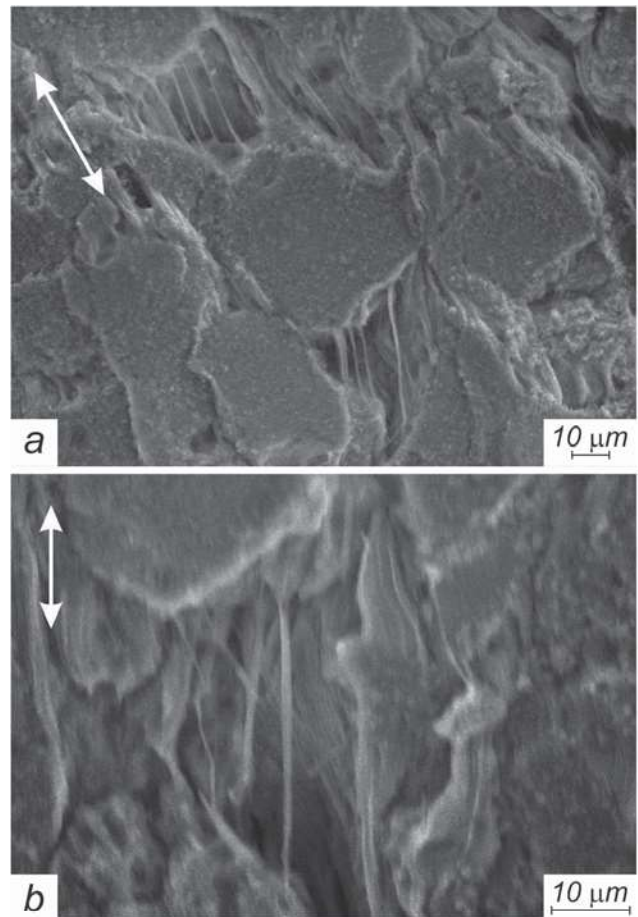


Fig.4. The deformation relief of alloy 1933 specimens, deformed to failure under the optimal conditions of high-temperature superplasticity. Scanning electron microscopy. Arrows indicate the tensile direction of specimens.

concentration of magnesium strongly indicate that this alloy shown HTSP in solid-liquid state.

Let us analyze the influence of the structural state and phase composition of the alloy 1933 on the development of deformational and accommodative mechanisms of its SPD.

Analysis of the specific views of deformation relief formed on the surface of superplastically deformed specimens, typical views of which are shown in Figure 5, and the use of previously obtained data on the contribution of GBS to the local deformation of its specimens [8-9] provides a basis to offer a qualitative description of the development of deformational and accommodative mechanisms of SPD of alloy 1933 with a bimodal structure.

We can assume that during superplastic flow of specimens of the alloys 1933, at the same time take place three main deformation mechanisms: GBS, intragranular deformation carried out due to sliding and climbing of lattice dislocations and diffusion creep.

In [18,19] considered the effect of the presence of a bimodal structure on the development of SPD of aluminum alloy 01570C specimens (Al – 5,0% wt. Mg – 0,18 % wt. Mn – 0,2 % wt. Sc – 0,8 % wt. Zr). It



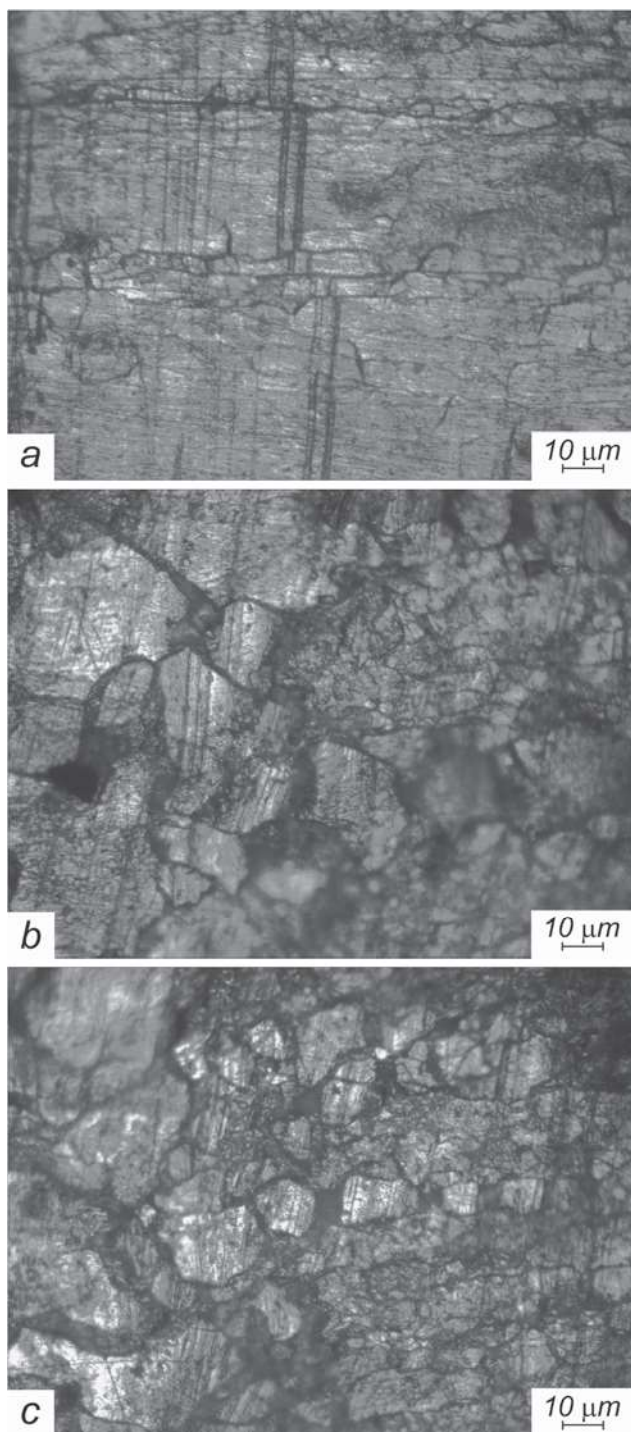


Fig. 5. Characteristic views of deformation relief formed on the surface of the working part of specimens of alloy 1933, deformed to failure under the optimal conditions of high-temperature superplasticity. The tensile direction is horizontal. Light microscopy.

is suggested that in the process of dynamic loading of the specimen initially large grains begin to deform. In this case intense flows of lattice dislocations generate, they fall on the HABs grains in a fine-grained structure, transfer them to a non-equilibrium state. This enables the development of GBS in the fine structure part of the alloy. Streams of lattice dislocations from volume of coarse grains activate

the overwhelming number of HABs grains. Under the influence of the dislocation stream excess nonequilibrium volume of HABs grains increases, and as a result, the diffusion processes in such boundaries are significantly more active, which leads to faster diffusion of HABs and the intensive development of GBS [1,18,19].

We can assume that in the specimens of studied 1933 alloy intragranular deformation of the alloy, which is used to create nonequilibrium state of HABs grains by applying stress to the specimen starts to be implemented simultaneously in large elongated polygonized grains, and in the fine and ultrafine grains in which the external stress in according to the Schmidt law, reaches a critical shear stress.

In [8,9], it was found that GBS in the specimens of alloy 1933 intensively take place at the grain boundaries, which consist of areas occupied by the solid and liquid phases.

Apparently, intense GBS on solid areas of HABs of ultrafine and fine grains takes place on the same micro-processes that are active in terms of manifestation of micro-grain SSP [1,2]. However, in consideration of deformation mechanisms of alloy 1933 is necessary to take into account that in specimens of aluminum alloys, superplastically deformed at high homologous temperatures, GBS may be further intensified by the separation of grain boundary dislocations from the impurity atoms on the atmospheres of ultrafine grain boundaries [20], as well as by substantially increasing diffusion processes at the boundaries of coarse grains [21].

Apparently, intense GBS occurring on the solid parts of HABs boundaries of large and of ultrafine grains, accompanied by the development of viscous flow in those areas of HABs and LABs of all the grains that contain a viscous liquid phase, which is a liquid-solid suspension. As a result, as shown in [9,10], GBS can intensively develop not only on the HABs of fine and ultrafine grains but also on LABs of coarse grains, including polygonized grains oriented parallel to the axis of tension of the specimen.

It was determined [9,10], that the contribution of GBS to the local deformation of the specimen due to the implementation of GBS in different parts of their working part is different. As shown estimate calculations [9,10], its values are within the range of  $\approx 50\%$  and  $\approx 80\%$ .

As shown in [22], the liquid phase, which borders with potential stress concentrators (intermetallic particles, triple junctions of grains and other structural inhomogeneities, which are available on the grain boundaries), promotes relaxation of local stresses arising during the GBS.

When at the intercrystalline boundaries there are areas occupied by the liquid-solid phase, the GBS on such boundaries can be facilitated as compared with sliding on "solid" boundaries.

In the specimens of investigated alloy 1933, this

process will be implemented under the action of shear stresses due to relative displacement of the layers of liquid-solid phase enriched by surface active elements, since, as specified in [22], in a case if the liquid phase is in the form of a film between the crystallites, the deformation capacity of the material shearing increases, and its peel strength is retained.

To ensure the stability of the SPD during superplastic flow of investigated specimens of alloy 1933, in their working part must the effectively different accommodative mechanisms within the grains and at their sliding boundaries must take place, as well as in the area of contact between the liquid and solid phases. Accommodation of GBS can be effectively implemented with the active development of lattice and grain boundary diffusion in the solid phase and diffusion in the liquid phase. Active implementation of accommodative processes in the specimens of investigated alloy 1933 superplastically deformed in a solid-liquid state, promotes the effective stress relaxation in difficult for GBS areas of grain boundaries. As a result of a coherent implementation of the above-mentioned deformational and accommodative processes in the working part of the specimens of studied in this paper alloy 1933 with a bimodal structure the intensive rearrangement of grains with grain boundary cavities takes place, which is accompanied by viscous flow of liquid-solid phase localized at grain boundaries.

It is determined that at the early stages of superplastic flow in the working part of the alloy 1933 specimens, under the influence of normal stress on the HABs grains perpendicular to the tension direction of specimens begin to form wedge-shaped cracks. In those areas of the working part of specimens in which a partial melting of the alloy did not take place or the amount of liquid phase was small, it entirely dissolved in solid phase to the beginning of deformation. Wedge-like cracks during GBS were transformed into individual grain boundary cavities, developing in accordance with the mechanism proposed in [23] for micro-grain SSP, which took place in the solid phase.

Those wedge-like cracks that were formed by the mutual sliding of grains, boundaries of which contained inclusions of liquid-solid phase will also be transformed into the individual grain boundary cavities. Fibrous structures begin to form and develop during this. The edges of the grains, perpendicular to the strain axis of the specimen, i.e., walls of the cavities and cracks in this case act as a sort of "holders" to which fibers formed as a result of viscous flow of liquid-solid material is "attached". Further development of cavities and cracks occur mainly due to GBS, which is carried by grains adjacent to cavities with a speed of grain boundary shift through solid sections of the boundaries, the growth rate of the fibrous structures during SPD of specimens of the alloys is probably close in magnitude to

the rates of the disclosure of long grain boundary in which they are formed. As follows from data presented in [24], the growth rate of deformational cavities and the local rate of SPD associated with the presence and participation of these cavities in the deformation process, on average is about twice higher than the overall rate of SPD of specimen. Obviously, that the same in order of magnitude is the rate of development of fibrous structures during SPD, i.e. the rate of so-called "microsuperplasticity" [25].

This work is done with partial support by the target complex program "Fundamental Problems of Creation of New Nanomaterials and Nanotechnologies", project №62/15-N.

### Conclusions

1. The initial structural state of industrial alloy 1933, which showed the effect of high-temperature structural superplasticity in a solid-liquid state is investigated. It is shown that the original structure of the alloy 1933 is bimodal.
2. The specific proportion of grain boundaries of different misorientation in the initial specimens of alloy 1933, prepared for mechanical testing is determined. It is found that the specific proportion of the low-angle boundaries of grains is 65.5%, while the proportion of high-angle boundaries of grains is 35.5%.
3. The influence of the initial structural state and phase composition of alloy 1933 on the development of grain-boundary sliding and other mechanisms of its superplastic deformation, carried out on grain boundaries of different misorientation, as well as in the core of ultrafine and coarse grains during high-temperature superplasticity is analyzed.
4. The mechanism of grain boundary sliding in the alloy 1933 with a bimodal structure, intensively carried out on high-angle boundaries of fine and ultra-fine grains, as well as on low-angle boundaries between coarse, including polygonized grains oriented parallel to the tensile axis of the specimen is considered.

1. I.I. Novikov, V.K. Portnoy. *Sverkhplastichnost metallov i splavov s ultramelkim zernom*. M.: Metallurgiya, (1981), 168s.
2. O.A. Kaybyshv. *Sverkhplastichnost promyshlennykh splavov*. M.: Metallurgiya, (1984), 264s.
3. *Superplastic Forming of Structural Alloys*, Ed. by N.E. Paton and C.H. Hamilton. The Metallurgical Society of AIME, San Diego, California, (1982), 312p.
4. V.N. Shcherba. *Pressovanie alyuminievyykh splavov*. M.: Intermetinzhiniring, (2001), 768s.
5. V.M. Beleckii, G.A. Krivov. *Alyuminievye splavy (sostav, svoystva, tekhnologiya, primeneniye) spravochnik / Pod obshei redakciei akademika RAN I.N. Fridlyandera*. K.: Kominteh. 2005, 315p.
6. V.I. Elagin, V.V. Zakharov, M.M. Drits. *Struktura i svoystva*

- splavov sistemy Al-Zn-Mg. M.: Metallurgiya (1982), 224s.
7. D.E. Pedun, V.P. Poyda, T.F. Sukhova, A.P. Samsonik, V.V. Litvinenko, E.L. Spiridonov. *Visnyk KhNU, seriya «Fizyka»*. **V.16**, №1019, 63 (2012).
  8. D.E. Pedun, V.P. Poyda, V.V. Bryukhovetskiy, A.V. Poyda, A.P. Kryshchal', T.F. Sukhova, A.L. Samsonik, V.V. Litvinenko, E.K. Spiridonov. *Metallofizika i noveyshie tekhnologii*, **V.34**, №10, 1397 (2012).
  9. V.P. Poyda, D.E. Pedun, V.V. Bryukhovetskiy, A.V. Poyda, R.V. Sukhov, A.L. Samsonik, V.V. Litvinenko. *FMM*, **V.114**, №9, 779 (2013).
  10. D.E. Pedun, V.P. Poyda, V.V. Bryukhovetskiy, A.V. Poyda, R.V. Sukhov, A.P. Kryshchal'. *Visnyk KhNU, seriya «Fizyka»*, **V.18**, №1075, 55 (2013).
  11. M. Mabuchi, H.G. Jeong, K. Hiraga, K. Higashi. *Interface Sci.* **V.4**, №3 – 4, 357 (1996).
  12. I.I. Novikov, V.K. Portnoy, V.S. Levchenko, A.O. Nikiforov. *Mater. Sci. Forum.* **Vol.243 – 245**, 463 (1997).
  13. V.P. Poyda, R.I. Kuznetsova, T.F. Sukhova, N.K. Tsenev and others. *Metallofizika*, **V.12**, №1, 44 (1990).
  14. S.A. Saltykov. *Stereometricheskaya metallografiya*. M.: Metallurgiya, (1976), 272 s.
  15. V.N. Varyukhin, E.G. Pashinskaya, A.V. Zavdoveev, V.V. Burkhovetskiy. *Vozmozhnosti metoda difraktsii obratnorasseyannykh elektronov dlya analiza struktury deformirovannykh materialov*. K.: Naukova dumka, (2014) 101s.
  16. C.L. Chen, M.J. Tan. *Mater. Sci. and Eng. A.*, **298**, 235 (2001).
  17. W.D. Cao, X.P. Lu, H. Conrad. *Acta Mater.*, **44**, №2, 697 (1996).
  18. T.G. Karnavskaya, E.V. Avtokratova, A.M. Bragov, M.V. Markushev, O.Sh. Sitdikov, V.N. Perevezentsev, M.Yu. Shcherban'. *Pis'ma v ZhTF*. **V.38**, V.13. 48 (2012).
  19. O.E. Mukhametdinova, E.V. Avtokratova, O.Sh. Sitdikov, M.V. Markushev *Vestnik Tomskogo GU*. **V.18**, I.4. 972 (2013).
  20. R.O. Kaybyshev, F.F. Musin. O «subsolidusnoy» sverkhplastichnosti. *DAN*, **V.373**, №2, 185 (2000).
  21. M.Yu. Gryaznov, V.N. Chuvil'deev, V.E. Kuzin, M.M. Myshlyayev, V.I. Kopylov. *Fizika tverdogo tela. Vestnik Nizhegorodskogo universiteta im. N.I. Lobachevskogo*. №6 (1). 49 (2011).
  22. Higashi K., Nieh T.G., Mabuchi M., Wadsworth J. *Scripta Met. et Mater.*, **V.32**, N7. 1079 (1995).
  23. R.I. Kuznetsova. *FMM*, **V.45**, I.3, 641. (1978).
  24. R.I. Kuznetsova, V.V. Bryukhovetskiy, V.P. Poyda, T.F. Sukhova. *Metallofizika i noveyshie tekhnologii*. **V.17**, №8, 64 (1995).
  25. W.J.D. Shaw., *Materials Letters*, **4**, 1 (1985).